Effects of traces of oxygen on Grimm-type glow discharges in argon†

Sohail Mushtaq,*[a] Edward B. M. Steers,[b] Juliet C. Pickering,[a] Tamara Gusarova,[b] Petr Šmíd[c] and Viktoria Weinstein[b]

Received 29th April 2010, Accepted 4th August 2010
DOI: 10.1039/c0ja00013b

We report results of studies using Fourier Transform Optical Emission Spectroscopy (FT-OES) to investigate the effects of added oxygen (0.04–0.8% v/v) on observed spectra from a Grimm-type glow discharge, generated in argon plasma with a pure iron sample. Significant changes in the sputter rate and the intensities of atomic lines of the carrier gas and sample in the presence of oxygen are discussed in detail; these changes are greater than those observed with Ar/H_2 and Ar/N_2 mixtures. A detailed study of spectral line profiles shows changes in self-absorption of Ar I lines due to O_2 and H_2 traces. The sputter rate for a given Ar/O_2 gas mixture is found not to be proportional to current.

1. Introduction

Analytical glow discharge (GD) optical emission spectrometry is a technique used for both the study of solid bulk materials and compositional depth profiling (CDP).[1,2] The primary objective of this technique is to obtain rapid and accurate results of elemental composition for the analysis of solid materials, essential for the development of new materials and surface coatings and for production quality control. It is already known that traces of molecular gases such as H_2 and N_2 can affect elemental analyses in glow discharge optical emission spectroscopy (GD-OES),[3–8] particularly in CDP applications.[9] Contamination by trace molecular gases through residual moisture or atmospheric gases may be less serious with modern clean instrumentation. However, gaseous elements can be present in the sample material as a constituent such as an oxide (Al_2O_3, SiO_2, Ti_2O_3, ZrO_2), hydride (TiH_2), polymers or SnO_2-based mixed oxide electrode[10] and the contribution of molecular gases from the natural composition of the sample can lead to substantial inaccuracy in analytical results.[9] These analytical errors may result from discrepancy in crater profiles, fluctuation in the electrical parameters or from changes in emission intensity of many atomic analytical lines commonly used in commercial Glow Discharge Spectrometry (GDS). Although the basic processes of excitation and ionisation occurring in GD are well understood, particularly in Ar,[11] the situation becomes more complex when traces of molecular gases are present. For good analytical practice, it is essential to know how these O_2, H_2 and N_2 traces affect the ionization and excitation processes, and hence the accuracy of results.

Previously published work[2–8] has shown that traces of hydrogen or nitrogen in the working gas (usually argon), introduced into the GD as a molecular gas or as a constituent in the sample, can have a substantial effect on the electrical characteristics, on the sputter rate and on the spectrum emitted. Previous studies[12,13] on oxygen as an impurity involved investigation of only one or two lines of each of a number of elements (the analytical lines frequently selected on a commercial GD-OES instrument). We have carried out the first multi-line study for oxygen as an impurity in GDS, using the high resolution vacuum UV (VUV) Fourier transform spectrometer (FTS) at Imperial College, London (IC),[14–16] allowing several hundred spectral lines to be investigated, including lines of Ar I, Ar II, Fe I, Fe II and O I.

In this paper we report and discuss how the atomic emission line intensities of both the sputtered material, iron in this case, and the argon carrier gas behave with controlled addition of oxygen. In order to gain an insight into the effect of oxygen addition (Ar/O_2 glow discharge), results are compared with the cases[3] of Ar/H_2 and Ar/N_2. The results for ionic emission lines will be presented in a subsequent paper.

Also, since the sample sputter rate affects the intensities of sample lines, controlled experiments investigating the change in sample sputter rate with the oxygen concentration in the glow discharge have been undertaken, and the resulting crater profiles have been measured and the results compared with those observed[3] with Ar/H_2 and Ar/N_2 mixtures. In general for measurements on oxide materials an rf source is normal, but to have exact information and flexible control of the discharge parameters, a direct current (dc) source and only pure metal samples were used for this work.

2. Experimental details

The effect of oxygen as an impurity on the analytical glow discharge was investigated by using the IC VUV-FTS with a free-standing Grimm-type glow discharge source running in dc excitation mode. The spectral range of the IC VUV-FTS (140–900 nm) together with its high resolution is ideally matched to the study of emission spectra of iron and argon glow discharges containing small quantities of oxygen. Fe I analytical lines lie in the visible and UV spectral regions, while strong and analytically important oxygen and argon atomic lines are in the near infrared region. The IC VUV-FTS was used for three wavelength ranges 200–300 nm, 295–590 nm and 450–900 nm, with Hamamatsu R166, IP28 and R928 photomultiplier tube detectors, respectively, and appropriate filters. The spectrometer resolution

[a]*Blackett Laboratory, Imperial College, London, SW7 2BW, UK. E-mail: s.mushtaq@imperial.ac.uk*
[b]*London Metropolitan University, North Campus, 166-220 Holloway Road, London, UK*
[c]*Nuclear Research Institute Rez plc, Czech Republic*

† This article is part of a themed issue highlighting the latest work in the area of Glow Discharge Spectroscopy, including the work presented at the International Glow Discharge Spectroscopy Symposium 2010, August 22–25, Albi, France.

 This journal is © The Royal Society of Chemistry 2011

chosen was from 0.055 cm^{-1} to 0.033 cm^{-1}. In most cases this was sufficient to resolve the line profiles allowing spectral line shapes to be observed. At this resolution any lines affected by blends could be seen in the majority of cases, and unambiguous identifications of lines could be made even when major changes in relative line intensities occur.

In the original source designed by W. Grimm[17] the diameter of the anode tube was 8 mm and typical operating conditions were 800 V and 80 mA. In current GD instrumentation the inner anode diameters of the source available are typically 8, 4, 2.5 and 1.0 mm; the results presented here were obtained using a 4 mm anode tube with 700 V and 20 mA, "standard" conditions for much analytical work. The discharge was operated in constant current–constant voltage mode, so the overall pressure had to be adjusted to maintain the required discharge voltage when a molecular gas was admixed. It is common practice to work with fixed voltage and current because extensive investigations have shown that pressure variations have substantially smaller effects on line intensities than the variations of the electrical parameters in the constant pressure mode.[8,18,19]

The plasma gas was supplied to the source *via* a mixing system using three mass flow controllers (MKS Instruments, Inc.) with different flow ranges: 800, 200 and 20 sccm (standard cubic centimetre per minute). Various oxygen concentrations (0.04%, 0.08%, 0.20%, 0.40% and 0.80% v/v) were used, obtained by mixing pure argon with a mixture of argon with 2 ($\pm$0.02) % v/v oxygen. The pressure was measured by a Baratron capacitance diaphragm gauge, (MKS Instruments, Inc.), with a pressure range up to 20 Torr, connected directly to the body of the glow discharge source. Stainless steel tubing was used for all gas connections; even so, traces of OH bands were sometimes observed in the spectra even when using pure argon, and therefore a liquid nitrogen cooled trap was installed on the gas inlet line to remove any possible moisture from the gas.

The source was viewed end-on and an image of the cathode was focused on the entrance aperture of the FTS with a magnesium fluoride lens. Each double-sided interferogram was recorded as a single scan lasting about three minutes. The interferograms were subsequently transformed and phase corrected by using the GREMLIN program[20] to yield the spectrum, typically containing several hundred spectral lines. The ratios of spectral line intensities recorded in different spectra were found by comparing the measured area under the line profiles.

To investigate the excitation processes involved for individual energy levels, the observed line intensity ratios I_{Ar+O_2}/I_{Ar} for individual lines are plotted against the total excitation energy of the upper state of the transition involved. I_{Ar+O_2} is the intensity of a particular line excited in an Ar/O_2 mixture and I_{Ar} is the intensity of the same line excited in pure argon under the same constant current–constant voltage conditions. This comparison of observed spectral line intensities was possible as the spectral response of the spectrometer did not vary over the time scale of these measurements. When plotting such graphs a large number of emission lines with the widest possible range of upper energy levels are included so that the changes produced by the presence of traces of molecular gas for the individual levels can be investigated in detail.[6] Such investigations have been carried out with oxygen traces, using, for the first time, a large number of spectral lines over a wide spectral range including 67 Fe I lines (between 200 and 450 nm) and 29 Ar I lines (19 lines between 700 and 900 nm, and 10 lines between 390 and 440 nm). Spectral lines were identified using literature data sources[21–23] ensuring that any blended lines could be excluded from this study.

Sputter rate measurements were carried out with the same pure iron (purity 99.5%, Goodfellow) plates as used for FTS experiments. Various non-overlapping areas of the sample, circular and 4 mm in diameter, were sputtered for a defined time in the glow discharge source at constant current–constant voltage (20 mA or 40 mA, 700 V). After each replacement of the sample, no gas was admitted into the source until the pressure had fallen below 0.02 Torr. Final evaluation of the sputter rates of iron at various concentrations of oxygen were undertaken by measuring the volume of craters on the sample surface using a Fries Research & Technology (FRT) optical depth profilometer (MicroProf) at Leibniz-Institut für Festkörper- und Werkstoffforschung (IFW) Dresden (Germany). The error in crater volume measurement was less than 10% at oxygen concentrations less than 0.2% v/v. However, at greater oxygen concentrations the crater depths were less than 10 μm and small irregularities on the sample surface led to larger errors, resulting in 20–50% uncertainty in the crater volume measurements for 0.8% v/v oxygen concentration. This gives 20–50% errors in the resulting derived sputter rates.

3. Results and discussion

The changes produced by the added oxygen in the intensities of the oxygen, argon and iron atomic emission lines and in sample sputter rates are each discussed separately in this section.

Behaviour of O I emission lines in the GD with Ar and trace O_2

All the observed spectra, generated in an Ar/O_2 discharge plasma with pure iron, include lines of the intense atomic oxygen O I ^5S–^5P multiplet (777.194, 777.416 and 777.538 nm). These lines, very close in wavelength, originate from upper energy levels lying around 10.740 eV.[24] In a modelling study on Ar/O_2 GD[25] Bogaerts has recently predicted the presence of a significant concentration of O (^3P) ground state atoms, about two orders of magnitude lower than that of O_2 (X) ground state molecules. The dissociation of O_2 by argon metastable atoms, Ar_m*,[26–29] and electron impact dissociation[30] are the dominant production processes of the O (^3P) atoms in Ar/O_2 GD. The other group of strong O I lines frequently used for analytical purposes lie in the VUV spectral region just below the lower wavelength limit (135 nm) of the range of the IC VUV FTS, and would also be subject to molecular absorption by the added oxygen in the source. No other O I lines with sufficient signal-to-noise ratio to be included in this work were observed.

Emission line intensity ratios of observed O I lines as a function of oxygen concentration are shown in Fig. 1. The emission intensities of these three O I lines increase as the oxygen concentration in the plasma gas increases, the change becoming non-linear at higher oxygen concentrations. The non-linearity in emission intensities could be partly due to self-absorption but the profiles of these lines do not show this effect. In addition the line strengths, and therefore the absorption coefficients, differ by a factor of more than two, so any self-absorption would affect lines by differing amounts and can therefore be ruled out. The

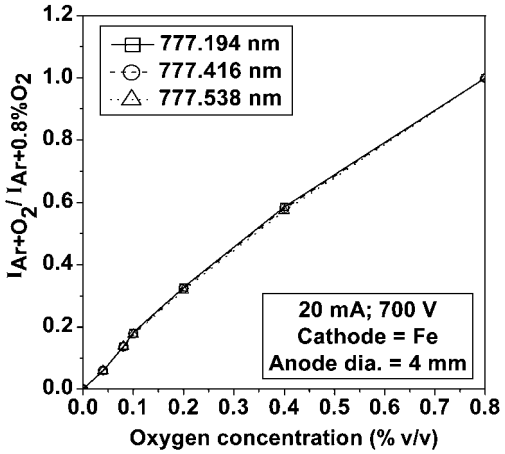

Fig. 1 Plots of the emission intensities of oxygen atomic lines, 777.194 nm, 777.416 nm and 777.538 nm, as a function of oxygen concentration, normalised to intensities measured with 0.80% v/v oxygen addition.

other possible explanation is a decrease in the degree of dissociation for higher oxygen concentrations as predicted by Bogaerts.[25]

Similar results have been reported for other molecular gases. Šmíd *et al.*[31] investigated the effect of nitrogen on Grimm-type glow discharges by using the high resolution IC FTS. All of the observed N I lines exhibited non-linear behaviour in emission intensities above ~0.15% v/v concentration, and Šmíd *et al.* suggest that changes in the degree of dissociation of nitrogen are responsible. In the case of hydrogen, Hodoroaba *et al.*[4] and Steers *et al.*[6] reported a non-linear increase in intensity of atomic hydrogen lines (486 nm and 656 nm) at higher H_2 concentrations. Thus, the behaviour of O I emission lines presented in this paper is in agreement with results for H_2 and N_2 molecular gases previously published.

Behaviour of Ar I emission lines in GD with Ar and trace O_2: intensities and line profiles

Prior to a detailed discussion of the investigation of differing behaviours of intensity ratios with oxygen and hydrogen addition, it is useful to discuss changes in observed line profiles with trace gas concentration for some emission lines affected by self-absorption.

The changes in the observed profiles of the Ar I 763.511 nm line when oxygen is added to the plasma gas is shown in Fig. 2a illustrating the large decrease in observed intensity produced by self-absorption. By contrast, the profiles of the Ar I 800.616 nm line (Fig. 2b) reveal no absorption effects. To demonstrate the changes in profile more clearly, Fig. 3 shows the normalised profiles of the 811.531 nm, 842.465 nm and 763.511 nm lines (4s–4p transitions) with the addition of oxygen and hydrogen, changes in self-absorption and self-reversal being clearly seen.

The changes in the Ar I line profiles with the trace gas addition are clearly due to self-absorption. Reduction in self-absorption occurs with increasing concentration of O_2 and H_2 in the argon plasma. These changes may be a result of quenching the population of the argon metastable level 4s $^2[3/2]_2$ or the loss of the electrons which are responsible for the excitation of these levels. For example, the population of argon metastable levels is known to be quenched by the addition of oxygen to pure argon due to dissociative excitation energy transfer into lower lying oxygen atoms.[26–29] The loss of electrons in the Ar/O_2 mixture may occur by dissociative recombination with O_2^+,[32] dissociative attachment of O_2,[25] or electrons may lose their energy by inelastic collisions with oxygen molecules.[32–34]

Šmíd *et al.*[31] also reported a change in self-absorption for the Ar I 811.531 nm line on the addition of N_2 in argon using 40 mA, 700 V discharge conditions with an 8 mm anode. Comparing the cases of O_2, H_2 and N_2 addition, the overall trend for self-absorption is similar, although it appears that changes in self-absorption, by quenching of Ar_m^*, due to O_2 are much more significant than those due to N_2. Moreover, the results presented here are in agreement with modelling studies by Bogaerts where more pronounced quenching of Ar_m^* due to O_2 addition has been reported[25] than for the case of N_2.[35]

Having discussed the effect of oxygen and hydrogen traces on Ar I line shapes, the behaviour of the Ar I emission lines with molecular gas addition can now be discussed in detail. The intensity ratios for 29 atomic argon emission lines (300–900 nm),

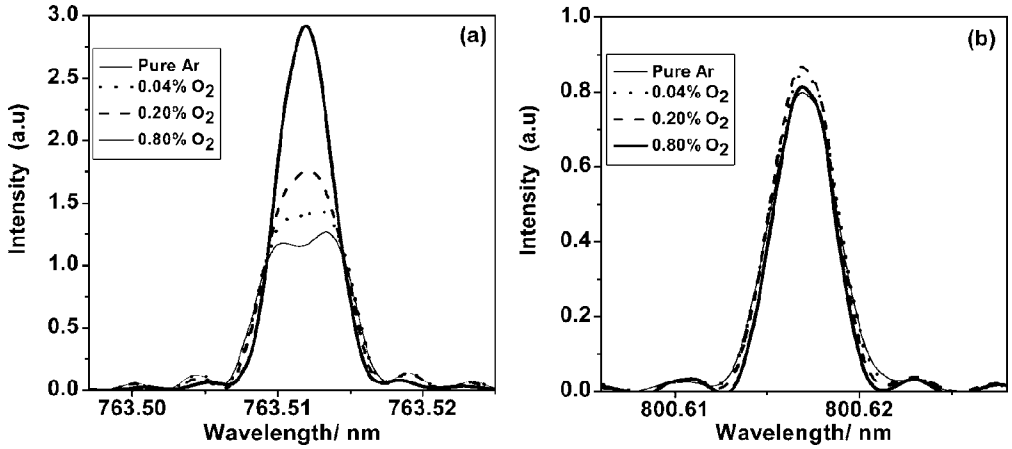

Fig. 2 Example of line profiles of (a) Ar I 763.511 nm, showing self-absorption and (b) Ar I 800.616 nm for various O_2 concentrations. Discharge conditions were 700 V, 20 mA for a 4 mm anode tube diameter.

 This journal is © The Royal Society of Chemistry 2011

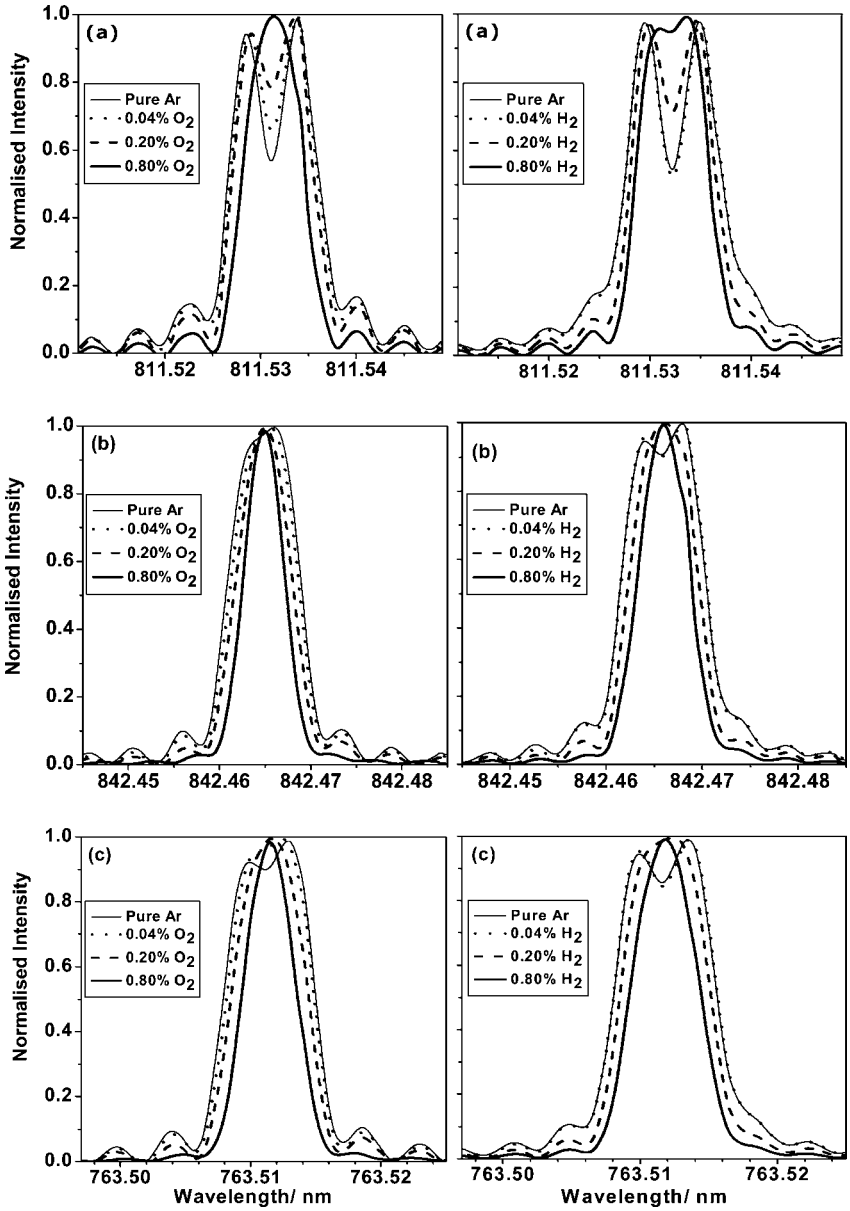

Fig. 3 Examples of normalised line profiles of argon lines: (a) 811.531 nm, (b) 842.465 nm and (c) 763.511 nm, showing self-absorption (in some cases self-reversal) for various O_2 and H_2 concentrations. Discharge conditions were 700 V, 20 mA for a 4 mm anode tube diameter. Note that slightly different resolutions were used for the experiments with oxygen (0.036 cm^{-1}) and hydrogen (0.033 cm^{-1}). "Ringing" is seen on either side of the line profile, as a result of insufficient resolution at these long wavelengths.

involving transitions from 4p and 5p energy levels, are plotted against excitation energy of the upper level of the transition in Fig. 4 in order to investigate the changes in line intensities by 0.04% v/v O_2 addition.

There are two groups of data points seen in Fig. 4, representing lines with excitation energy ~13.0–13.5 eV and ~14.4–14.8 eV. The 4s–4p transitions, in spectral region 700–900 nm, are the most intense of the observed Ar I lines. The 4s–5p transitions, in spectral region 390–440 nm, are relatively weak compared to the 4s–4p transitions,[11] and thus have higher errors in intensity ratios due to lower signal-to-noise ratio in the observed spectra.

For a more detailed look into the processes occurring, the intensity ratios of selected argon atomic lines from differing excitation energy ranges for various O_2 concentrations and their comparison with newly measured intensity ratios for the same set of lines with an Ar/H_2 mixture are presented in Fig. 5 and Fig. 6. For both Ar/O_2 and Ar/H_2 mixtures, the same electrical parameters were used; the changes in total gas pressure with progressive addition of oxygen and hydrogen into the argon plasma are given in Table 1. Details of the Ar I transitions are given in Table 2.

In general, the excitation processes responsible for populating the Ar I upper levels vary in different locations in the plasma.[36,37] The presence of oxygen may affect excitation processes by altering the number density and spatial distribution of electrons, argon ions and argon metastables and the population of excited levels of argon.[25] Also, reduction in self-absorption with

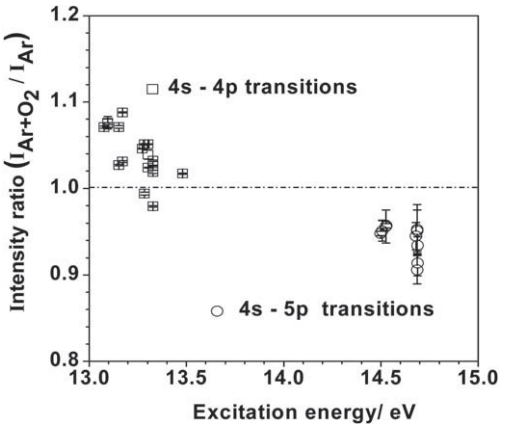

Fig. 4 Intensity ratios for argon atomic lines measured in Ar + 0.04% v/v O_2 and pure Ar as a function of their excitation energy for 700 V and 20 mA.

the addition of O_2, discussed above, is responsible for significant changes in observed intensity ratio of Ar I emission lines.

In the case of Ar/O_2 mixtures, the majority of the intensity ratios for lines within the excitation energy range ~13.0–13.5 eV are observed to increase with very low oxygen concentration 0.04% v/v. At the same time, the overall pressure had to be decreased (see Table 1) to maintain the voltage and current at the constant values. At higher oxygen concentrations, several features can be seen. A clear increasing trend is apparent in the intensity ratios of the Ar I lines 811.531 nm, 801.479 nm and 842.465 nm (excitation energy between 13.0–13.1 eV) with increasing O_2 concentration. For the Ar I lines 763.511 nm and 800.616 nm differing behaviour is observed. These two transitions originate from the same upper energy level, 13.172 eV; however, the lower energy level of the 763.511 nm transition is metastable. The drop in intensity ratio with increasing added oxygen concentration for the 800.616 nm line shows that the

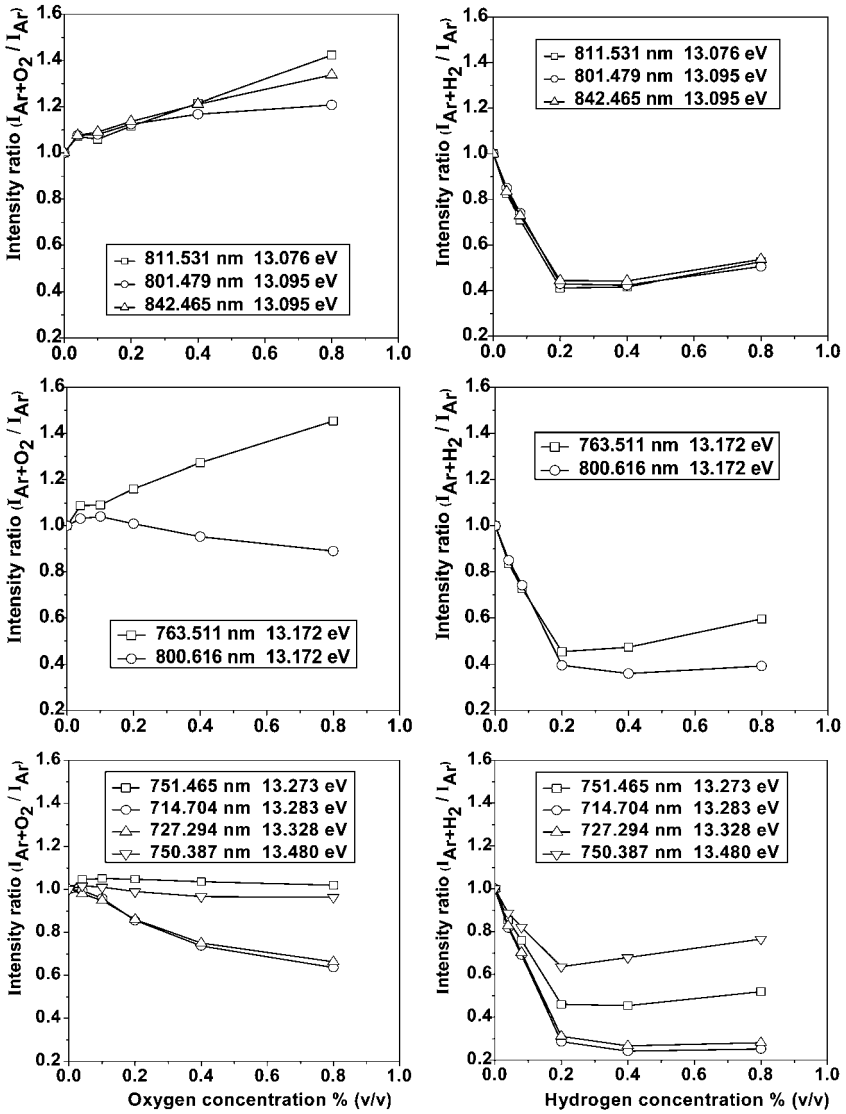

Fig. 5 Intensity ratios of selected argon atomic lines (excitation energy ~13.0–13.5 eV) measured at 700 V and 20 mA plotted against various oxygen and hydrogen concentrations.

 This journal is © The Royal Society of Chemistry 2011

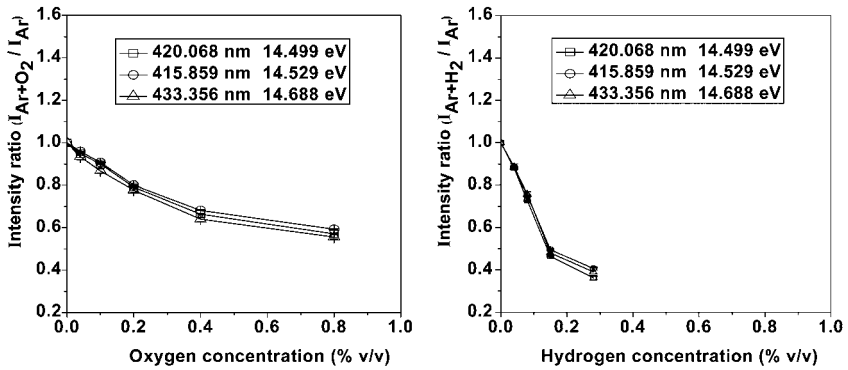

Fig. 6 Intensity ratios of selected argon atomic lines (excitation energy ~14.4–14.8 eV) measured at 700 V and 20 mA plotted against various oxygen and hydrogen concentrations.

Table 1 Variations of the gas pressure during the experiments in Ar/O_2 and Ar/H_2 with iron samples at constant dc electrical parameters (20 mA and 700 V) in GD

Ar/O_2		Ar/H_2	
O_2 Concentration (% v/v), ± 5%	Pressure (Torr) ± 0.02	H_2 Concentration (% v/v) ± 5%	Pressure (Torr) ± 0.02
0	5.96	0	6.42
0.04	5.92	0.04	6.90
0.08	5.80	0.08	7.40
0.20	5.84	0.20	7.68
0.40	5.82	0.40	8.04
0.80	6.10	0.80	8.10

population of the upper level must be reduced, however, for the 763.511 nm transition we find (Fig. 2a) that this effect is masked by the reduction in self-absorption caused by the added oxygen as discussed earlier, giving a net increase in intensity ratio. Both Ar I lines 801.479 nm and 842.465 nm, originating from the same upper energy level 13.095 eV, show an increase in intensity ratios, even though the lower energy level of Ar I 842.465 nm is not metastable. This can be understood by considering that the transition probability (see Table 2) of the 842.465 nm line is significantly higher than that of 801.479 nm, and thus the 842.465 nm line is more affected by the reduction of self-absorption with increase in oxygen concentration, contributing to the enhancement of its intensity (see Fig. 3 and Fig. 5).

However, for the Ar I lines 714.704 nm and 727.294 nm (with excitation energy in range 13.28–13.40 eV) the intensity ratios decrease with increasing O_2 concentration. It can be seen from Fig. 4 that the intensity ratios of all the lines corresponding to transitions from 5p levels, decrease with increasing O_2 concentration at a much higher rate than those of lines from 4p levels. Intensity ratios of some selected example Ar I emission lines against oxygen concentration are shown in Fig. 6.

In the case of an Ar/H_2 mixture the intensity ratios of the Ar I lines initially decrease at lowest H_2 concentration 0.04% v/v. The decrease becomes less pronounced at H_2 concentrations above 0.2% v/v, for most observed Ar I lines even a slight increase of intensity ratio with higher H_2 concentrations could be seen. From Fig. 5 and 6 one sees that the effect of oxygen addition on intensity ratios of emission lines is much more varied than in the case of hydrogen addition. On hydrogen addition all observed lines (see Fig. 5 & 6) behave in approximately similar ways independent of their excitation energy. One of the possible explanations for the differing behaviour of intensity ratios in Ar/O_2 and Ar/H_2 mixtures could be significantly higher pressure in the case of hydrogen addition. The increase in pressure needed to maintain constant

Table 2 The Ar I emission lines discussed in this paper with details of the transitions (from ref. 23 and 40) and approximate relative intensities as recorded in this work.[a]

				Configurations				
λ/nm	I_{line}[b]	Lower energy/eV	Upper energy/eV	Lower	Upper	Terms	J_i–J_k[c]	A[d]/10^6 s^{-1}
811.531	M	**11.548**	13.076	$3s^23p^5(^2P_{3/2})4s$	$3s^23p^5(^2P_{3/2})4p$	$^2[3/2]^o$-$^2[5/2]$	2–3	33.1
801.479	M	**11.548**	13.095	$3s^23p^5(^2P_{3/2})4s$	$3s^23p^5(^2P_{3/2})4p$	$^2[3/2]^o$-$^2[5/2]$	2–2	9.28
842.465	W	11.624	13.095	$3s^23p^5(^2P_{3/2})4s$	$3s^23p^5(^2P_{3/2})4p$	$^2[3/2]^o$-$^2[5/2]$	1–2	21.5
763.511	S	**11.548**	13.172	$3s^23p^5(^2P_{3/2})4s$	$3s^23p^5(^2P_{3/2})4p$	$^2[3/2]^o$-$^2[3/2]$	2–2	24.5
800.616	M	11.624	13.172	$3s^23p^5(^2P_{3/2})4s$	$3s^23p^5(^2P_{3/2})4p$	$^2[3/2]^o$-$^2[3/2]$	1–2	4.90
751.465	S	11.624	13.273	$3s^23p^5(^2P_{3/2})4s$	$3s^23p^5(^2P_{3/2})4p$	$^2[3/2]^o$-$^2[1/2]$	1–0	40.2
714.704	M	**11.548**	13.283	$3s^23p^5(^2P_{3/2})4s$	$3s^23p^5(^2P_{1/2})4p$	$^2[3/2]^o$-$^2[3/2]$	2–1	0.62
727.294	M	11.624	13.328	$3s^23p^5(^2P_{3/2})4s$	$3s^23p^5(^2P_{1/2})4p$	$^2[3/2]^o$-$^2[1/2]$	1–1	1.83
750.387	VS	11.828	13.479	$3s^23p^5(^2P_{1/2})4s$	$3s^23p^5(^2P_{1/2})4p$	$^2[1/2]^o$-$^2[1/2]$	1–0	44.5
420.068	M	**11.548**	14.499	$3s^23p^5(^2P_{3/2})4s$	$3s^23p^5(^2P_{3/2})5p$	$^2[3/2]^o$-$^2[5/2]$	2–3	0.93
415.859	M	**11.548**	14.529	$3s^23p^5(^2P_{3/2})4s$	$3s^23p^5(^2P_{3/2})5p$	$^2[3/2]^o$-$^2[3/2]$	2–2	1.40
433.356	W	11.828	14.688	$3s^23p^5(^2P_{1/2})4s$	$3s^23p^5(^2P_{1/2})5p$	$^2[1/2]^o$-$^2[3/2]$	1–2	0.55

[a] Note: The metastable level: $3s^23p^5(^2P_{3/2})4s$ (11.548 eV) is indicated by bold numbers. [b] I is the observed line intensity; VS = very strong; S = strong; M = medium and W = weak. [c] k is for upper state and i is for lower state. [d] A is the transition probability.[40]

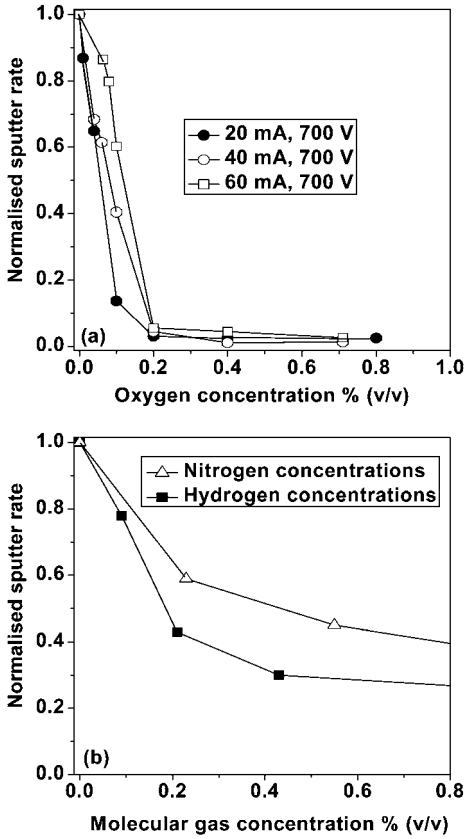

Fig. 7 Normalised sputter rate for iron as a function of the molecular gas concentration: (a) O_2 addition, at (●) 700 V, 20 mA (○) 700 V, 40 mA and (□) 700 V, 60 mA in 4 mm anode tube; (b) H_2 (■) and N_2 (△) addition, at 700 V, 40 mA in 8 mm anode tube, reproduced from ref. 3 by permission of The Royal Society of Chemistry. It should be noted that in Fig. 7(a) at low sputter rate even the large uncertainty of ~50% gives error bars smaller than symbols.

electrical parameters with progressive addition of hydrogen (see Table 1) is more than that needed for oxygen and this may well affect the excitation and ionization processes.

Effect on the sputter rate of trace molecular gas addition to argon glow discharge

Šmíd *et al.* measured the sputter rate of iron and titanium as a function of H_2 and N_2 concentration at 700 V, 40 mA in 8 mm anode tube in an Ar GD.[3] They observed that the sputter rate decreases with increasing concentration of H_2 and N_2 in GD. In our study, controlled experiments investigating the change in iron (sample) sputter rate with O_2 concentration in the GD have been undertaken, and the resulting crater profiles were used to measure sputter rate. These measured sputter rates were normalised to those obtained in pure Ar (Fig. 7(a)) and compared with normalised sputter rates for iron in Ar/H_2 and Ar/N_2 (Fig. 7(b)) reproduced from Šmíd *et al.*[3]

From Fig. 7 it is clear that the sputter rate of iron decreases very significantly with increasing O_2 concentration, even at very low O_2 concentrations of 0.04% v/v and 0.10% v/v, much more than in the case of increasing H_2 and N_2 concentration. This

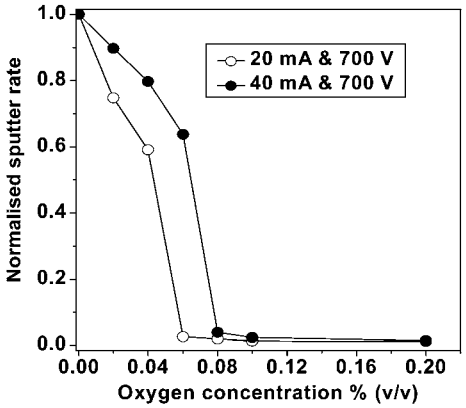

Fig. 8 Normalised sputter rate for Ti as a function of O_2 addition, at (●) 700 V, 20 mA and (○) 700 V, 40 mA in 4 mm anode tube.

effect can be attributed to the formation of an oxide layer on the cathode surface due to the bombardment of oxygen species. This "poisoning" of the cathode surface is also well known in reactive magnetron sputtering.[3,25] Similarly a sudden drop in the sputter rate was observed in the case of titanium when sputtered in Ar/N_2,[3] probably due to poisoning of the Ti surface and formation of titanium nitrides. Sputter rate measurements at higher oxygen concentrations show no further decrease, so it appears that the formation of the oxide layer is complete.

Furthermore, during experiments it was observed that in the case of pure Ar the eroded area of the cathode appeared whitish with a silver shine, however, with Ar/O_2 mixtures the area seemed to be covered with a brown powder. This indicates the formation of an iron oxide as a thin surface layer on the cathode (iron sample).

An important result obtained is that the sputter rate for a given Ar/O_2 gas mixture appears to be not always proportional to the GD current, the usual assumption for GDS. The Boumans equation[38] suggests that if the voltage remains constant, the sputter rate should be proportional to current, however, in studies on the effect of a small addition of O_2, with an iron sample and argon gas, a different trend has been observed (Fig. 7(a)) probably due to "poisoning" of the cathode surface, *i.e.* a different material is being sputtered rather than a breakdown in the Boumans equation. This effect is more pronounced for titanium samples, see Fig. 8, where results of sputter rate measurements for 700 V, 20 & 40 mA with various oxygen concentrations are shown. The effect of trace oxygen to GD with Ti sample will be discussed in a future paper.

Behaviour of Fe I emission lines in GD with addition of O_2 traces

67 Fe I emission lines are used to investigate the effect of O_2 addition on sample emission lines and are presented in Fig. 9.

Since the presence of O_2 reduces the sputter rate, a large part of the reduction in the Fe I line intensity ratios with O_2 addition is caused by the decrease in the iron atom population in the plasma, leading to a decrease in the observed intensity of Fe I emission lines. The more oxygen is added to discharge gas, the smaller the measured intensity ratios.

 This journal is © The Royal Society of Chemistry 2011

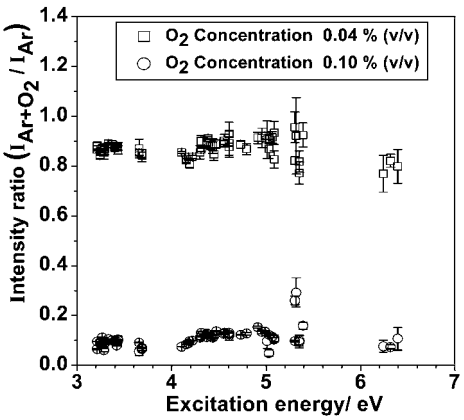

Fig. 9 Intensity ratios of 67 Fe I lines as a function of their excitation energy for 700 V and 20 mA (anode tube dia. 4 mm) for two oxygen concentrations (0.04 and 0.10% v/v).

The rapid decrease in the sputter rate with increasing oxygen concentration makes a detailed study of the effect of oxygen on the population of upper energy levels of a large number of Fe I transitions complicated. Therefore, it is necessary to keep in mind changes in sputter rates when considering intensity changes for different oxygen concentrations. Correcting a particular line for sputter rate changes, by dividing the intensity by the sputter rate and concentration of analyte in the matrix [100% in this case], gives a quantity known as emission yield (EY), which, if used instead of measured intensity, gives a more realistic picture of differences in excitation processes. More details about emission yields and the standard model in GD-OES are given by Weiss.[39]

In Fig. 10, the EY ratios of iron atomic emission lines are plotted against the upper level excitation energies, for three different oxygen concentrations. Here EY_{Ar+O_2} is the relative intensity of a particular line corrected for sputter rate in an Ar/O_2 mixture, and EY_{Ar} is the intensity of the same line corrected for sputter rate in pure argon. Intensity ratios are decreased due to reduced sputter rate by progressive addition of oxygen (Fig. 9) but, after correcting for sputter rate, some emission yield ratios show a slight increase (Fig. 10) which can be explained by enhanced excitation when oxygen is added in pure argon. The results shown in Fig. 10(c) were obtained with higher oxygen concentration and therefore the effect of the excitation enhancement is more pronounced and the differences between the various levels become greater. The overall variation in the intensity ratio with upper level excitation energy indicates that different excitation processes, such as electron impact, fast argon ion and atom impact excitation, in different areas of the GD, responsible for populating the upper levels, are affected by the addition of oxygen.

Similar to Ar I emission lines, Fe I line profiles have been investigated for a discharge in pure argon and different Ar/O_2 mixtures. Self-reversal was only observed for the Fe I 248.327 nm line and this was reduced by the progressive addition of oxygen in argon GD. The transition probability of the Fe I 248.327 nm emission line (see Table 3) is considerably higher than that of the other selected Fe I emission lines. The Fe I 248.327 nm line is one of the intense emission lines in the iron spectrum and should be avoided for any analytical applications or the study of plasma characterisation.

In Fig. 11 EY ratios of selected Fe I lines are plotted, showing the effects of oxygen and hydrogen addition on the excitation processes for various upper energy levels. The Fe I lines have been selected so that a wide range of differing excitation energies is investigated, (Fig. 10). As noted previously, for oxygen concentration $\geq$0.20% v/v the absolute value of the sputter rate and therefore EY is subject to a large error (20–50%), however, since the same sputter rate is used for all lines for a particular oxygen concentration, the differences in behaviour of the lines for the given oxygen concentration is not subject to this error. Details of all the selected lines are given in Table 3. The intensity of the Fe I 281.329 nm line is strongly enhanced in the presence of oxygen. Šmíd *et al.*[3] earlier reported that similar effects occurred for this line in Ar/H_2 mixtures whereas no such effect was observed for Ar/N_2. Also Ti I lines with upper energies ~5.3 eV did not show a similar marked effect in Ar/H_2 mixtures. The new measurements (Fig. 11b) confirm the effect with Ar/H_2. The reason for the enhancement of this line (Fe I 281.329 nm) is not yet understood, but may be explained in the future as part of a planned comparison of the atomic spectra behaviour for various elements in Ar/O_2 mixtures.

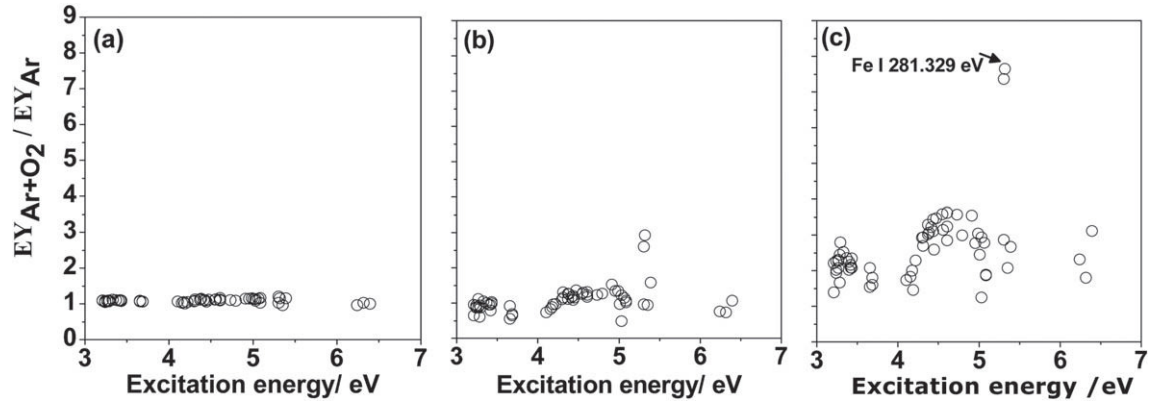

Fig. 10 Emission yields (EY) of Fe I lines as a function of their excitation energy for 700 V and 20 mA for (a) 0.04 (b) 0.10 and (c) 0.20% v/v oxygen concentrations. Errors in the measured sputtered rate (less than 10%) will affect all points in the same way.

Table 3 The Fe I emission lines discussed in this paper with details of the transitions (from ref. 3, 21 and 41) and approximate relative intensities as recorded

				Configurations				
λ/nm	I_{line}[a]	Lower energy/eV	Upper Energy/eV	Lower	Upper	Terms	J_i–J_k[b]	A[c]/10^7 s^{-1}
385.991	S	0.000	3.211	$3d^6 4s^2$	$3d^6(^5D)4s4p(^3P)$	^5D-$^5D^o$	4–4	0.96
371.993	S	0.000	3.332	$3d^6 4s^2$	$3d^6(^5D)4s4p(^3P)$	^5D-$^5F^o$	4–5	1.65
382.782	M	1.557	4.795	$3d^7(^4F)4s$	$3d^7(^4F)4p$	^3F-$^3D^o$	3–2	11.3
248.327	S	0.000	4.991	$3d^6 4s^2$	$3d^6(^5D)4s4p(^1P)$	^5D-$^5F^o$	4–5	48.1
281.329	W	0.915	5.320	$3p^6 3d^7(^4F)4s$	$3d^6(a^3F)4s4p(^3P)$	^5F-$^5G^o$	4–5	3.42
355.493	W	2.833	6.320	$3d^6(^5D)4s4p(^3P)$	$3d^6(^5D)4s(^6D)4d$	$^7F^o$-^7G	5–6	14.0

[a] I is the observed line intensity; S = strong; M = medium and W = weak. [b] k is for upper state and i is for lower state. [c] A is the transition probability.[41]

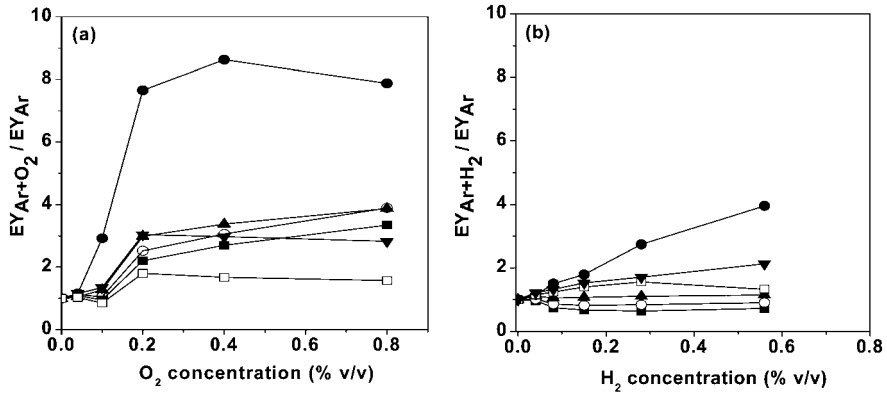

Fig. 11 Plots of emission yield ratio against (a) O_2 and (b) H_2 concentration for 700 V and 20 mA for selected Fe I lines: ■ Fe I 385.991 nm, 3.211 eV, ○ Fe I 371.993 nm, 3.332 eV, ▲ Fe I 382.782 nm, 4.795 eV, ▼ Fe I 248.327 nm, 4.991 eV, ● Fe I 281.329 nm, 5.320 eV, □ Fe I 355.493 nm, 6.320 eV. Note: The low sputter rate at O_2 concentrations greater than 0.20% v/v gives rise to an error of ~20–50% in the absolute value of the EY ratio; although this will not affect the differences in the behaviour shown by various spectral lines for the same O_2 concentration, this error should be borne in mind when comparing EYs for the lines at different O_2 concentrations.

4. Conclusion

Preliminary studies of the effect of oxygen in argon glow discharge plasma with a pure iron sample over a wide spectral range, including many emission lines of both the gas and sputtered material, have been undertaken. Major changes in the line intensities in emission spectra of iron and argon are observed when O_2 is present even in concentrations as low as ~0.04% v/v in the GD source. The decrease in self-absorption is clearly seen in selected Ar I line profiles with the addition of oxygen and hydrogen. The results presented here are in good agreement with the modelling studies on Ar/O_2 GD.[25] The effect of O_2 addition on the atomic argon emission lines was shown to be more complex than in the case of H_2 traces. Behaviour of emission lines resulting from different transitions and having different excitation energies was discussed in detail. Considerable enhancement of some argon atomic lines with total excitation energies of between ~13.0–13.2 eV in the presence of O_2 is observed. The 751.465 nm and 750.387 nm Ar I lines, by contrast, showed only a slight change in intensity ratio with increasing O_2 concentration. In general, the populations in 4p levels decrease slightly with the addition of oxygen though for many lines the effect is masked by major reductions in self absorption. The populations of 5p states also decrease, but at a more rapid rate.

The intensities of atomic iron emission lines were decreased due to suppression of sputter rates. Nevertheless, when comparing the emission yields the excitation of many Fe I emission lines was shown to be somewhat enhanced in presence of O_2.

It is found that the sputter rate for a given Ar/O_2 gas mixture is not proportional to current, usually the correct assumption in glow discharge work. It is clear that the sputter rate for iron drops very significantly with O_2 addition, much more than is the case with H_2 and N_2 addition, giving a rapid decrease in intensity of Fe I emission lines with increasing trace gas concentration. This appears to be due to a poisoning effect *e.g.* the formation of an oxide layer on the cathode surface. The changed surface means that this does not imply a breakdown of the Boumans equation; however, users should be aware that under these conditions, the sputter rate is not proportional to current.

Further experiments are planned investigating the effect of oxygen addition on the atomic spectra of other cathode materials in Ar GD, and also on the ionic lines (*e.g.* Fe II and Ar II) in comparison with GD-MS results.

Acknowledgements

The authors acknowledge the financial support from the European Union Analytical Glow Discharge Research Training

 This journal is © The Royal Society of Chemistry 2011

Network "GLADNET", contract no. MRTN-CT-2006-035459. The authors also thank Dr Volker Hoffmann, Dr Denis Klemm and Varvara Efimova for experimental support with measurements at IFW Dresden of sample crater volumes used in this work.

References

1 J. Angeli, A. Bengtson, A. Bogaerts, V. Hoffmann, V.-D. Hodoroaba and E. B. M. Steers, *J. Anal. At. Spectrom.*, 2003, **18**, 670–679.
2 A. Bengtson and S. Hänström, *ISIJ Int.*, 2002, **42**, 82–86.
3 P. Šmíd, E. B. M. Steers, Z. Weiss, J. C. Pickering and V. Hoffmann, *J. Anal. At. Spectrom.*, 2008, **23**, 1223–1233.
4 V. –D. Hodoroaba, V. Hoffmann, E. B. M. Steers and K. Wetzig, *J. Anal. At. Spectrom.*, 2000, **15**, 951–958.
5 V.-D. Hodoroaba, V. Hoffmann, E. B. M. Steers and K. Wetzig, *J. Anal. At. Spectrom.*, 2000, **15**, 1075–1080.
6 E. B. M. Steers, P. Šmíd and Z. Weiss, *Spectrochim. Acta, Part B*, 2006, **61**, 414–420.
7 B. Fernández, N. Bordel, C. Pérez, R. Pereiro and A. Sanz-Medel, *J. Anal. At. Spectrom.*, 2002, **17**, 1549–1555.
8 E. B. M. Steers, P. Šmíd, V. Hoffmann and Z. Weiss, *J. Phys. Conf. Ser.*, 2008, **133**, 012020.
9 A. Bengtson, *Spectrochim. Acta, Part B*, 2008, **63**, 917–928.
10 R. K. Marcus and J. A. C. Broekaert, *Glow Discharge Optical Emission Spectrometry*, J. Wiley, New York, 2003.
11 A. Bogaerts, R. Gijbels and J. Vlcek, *Spectrochim. Acta, Part B*, 1998, **53**, 1517–1526.
12 W. Fischer, W. Naoumidis and H. Nickel, *J. Anal. At. Spectrom.*, 1994, **9**, 375–380.
13 B. Fernández, N. Bordel, R. Pereiro and A. Sanz-Medel, *J. Anal. At. Spectrom.*, 2003, **18**, 151–156.
14 A. P. Thorne, U. Litzén, and S. Johansson, *Spectrophysics: Principles and Applications*, Springer Verlag, 1999.
15 A. P. Thorne, C. J. Harris, I. Wynne-Jones, R. C. M. Learner and G. Cox, *J. Phys. E: Sci. Instrum.*, 1987, **20**, 54–60.
16 J. C. Pickering, *Vib. Spectrosc.*, 2002, **29**, 27–43.
17 W. Grimm, *Spectrochim. Acta, Part B*, 1968, **23**, 443–454.
18 A. Bengtson and T. Nelis, *Anal. Bioanal. Chem.*, 2006, **385**, 568–585.
19 A. Bengtson, *Spectrochim. Acta, Part B*, 1985, **40**, 631–639.
20 J. W. Brault, *Mikrochim. Acta (Wien)*, 1987, **III**, 215–227.
21 G. Nave, S. Johansson, R. C. M. Learner, A. P. Thorne and J. W. Brault, *Astrophys. J. Suppl.*, 1994, **94**, 221–459.
22 G. Nave, R. C. M. Learner, A. P. Thorne and C. J. Harris, *J. Opt. Soc. Am. B*, 1991, **8**, 2028–2041.
23 W. Whaling, W. H. C. Anderson and M. T. Carle, *J. Res. Natl. Inst. Stand. Technol.*, 2002, **107**, 149–169.
24 S. J. Northway and R. C. Fry, *Appl. Spectrosc.*, 1980, **34**, 332–338.
25 A. Bogaerts, *Spectrochim. Acta, Part B*, 2009, **64**, 1266–1279.
26 L. G. Piper, J. E. Velazco and D. W. Sester, *J. Chem. Phys.*, 1973, **59**, 3323–3340.
27 W. R. Bennett, Jr, W. L. Faust, R. A. McFarlane and C. K. N. Patel, *Phys. Rev. Lett.*, 1962, **8**, 470–473.
28 G. Schaefer and H. Kirkici, *IEEE J. Quantum Electron.*, 1990, **26**, 1418–1424.
29 J. E. Velazco, J. H. Kolts and D. W. Setser, *J. Chem. Phys.*, 1978, **69**, 4357–4373.
30 B. Eliasson and U. Kogelschatz, *J. Phys. B: At. Mol. Phys.*, 1986, **19**, 1241–1247.
31 P. Šmíd, E. B. M. Steers, Z. Weiss and J. Vlcek, *J. Anal. At. Spectrom.*, 2003, **18**, 549–556.
32 S. Rauf and M. J. Kushner, *J. Appl. Phys.*, 1997, **82**, 2805–2813.
33 O. P. Makarov, I. Kanik and J. M. Ajello, *J. Geophys. Res.*, 2003, **108**, 1–11.
34 S. Tinck, W. Boullart and A. Bogaerts, *J. Phys. D: Appl. Phys.*, 2009, **42**, 095204.
35 A. Bogaerts, *Spectrochim. Acta, Part B*, 2009, **64**, 126–140.
36 P. Šmíd, E. B. M. Steers and V. Hoffmann, *Publ. Astron. Obs. Belgrade*, 2008, **84**, 325–329.
37 A. Bogaerts, Z. Donko, K. Kutasi, G. Bano, N. Pinhao and M. Pinheiro, *Spectrochim. Acta, Part B*, 2000, **55**, 1465–1479.
38 P. W. J. M. Boumans, *Anal. Chem.*, 1972, **44**, 1219–1228.
39 Z. Weiss, *Spectrochim. Acta, Part B*, 2006, **61**, 121–133.
40 W. L. Wiese, J. W. Brault, K. Danzmann, V. Helbig and M. Kock, *Phys. Rev. A: At., Mol., Opt. Phys.*, 1989, **39**, 2461–2471.
41 T. R. O'Brian, M. E. Wickliffe, J. E. Lawler, W. Whaling and J. W. Brault, *J. Opt. Soc. Am. B*, 1991, **8**, 1185–1201.